19th International Conference on
TRANSPORT AND SEDIMENTATION OF SOLID PARTICLES
24-27 September 2019, Cape Town, South Africa

MATHEMATICAL ANALYSIS OF CHANNELISATION IN NON-NEWTONIAN LAMINAR DEPOSITION FLOW

Arno Talmon

Delft University of Technology & Deltares, Mekelweg 2, 2628 CD, Delft, The Netherlands, a.m.talmon@tudelft.nl, arno.talmon@deltares.nl.

Channel formation is a common feature in the deposition of tailings. It is unknown how this initiates. It is investigated if channel formation in laminar flow can originate from hydrodynamics only. An analytical linearised approach is followed in order to establish a theoretical basis and a reference for further developments. It shows that thixotropy can govern pattern formation. Observations in tailings deposition flume testing are applied for reference. It is concluded that sidewall friction influences system behaviour in a similar way, and is here held responsible for meandering.

KEY WORDS: hydrodynamics, tailings, rheology, thixotropy, pattern formation.

NOTATION

a, b	complex wave parameters (1/m, 1/s)
g	gravitational acceleration (m/s^2)
h, u, v	local mud depth, local velocities (m, m/s, m/s)
h_0,u_0	mean value of mud depth and velocity (m, m/s)
h',u',v'	local variation of mud depth and velocity (m , m/s, m/s)
h˜,u˜,v˜	complex amplitude of perturbations (-)
i	complex number = √-1 (-)
i	ground slope (-)
L_x,L_y	wave length longitudinal &, transverse harmonic perturbations (m, m)
m	wave-number of transverse harmonic perturbations (1/m)
n	sensitivity τ for velocity variations (also: exponent power law) (-)
S	dimensionless horizontal viscosity (-)
t	time (s)
x, y	longitudinal and transverse coordinate (m, m)
τ	bed shear stress (Pa)
τ_0, τ'	mean & variation of bed shear stress (Pa)
τ_{xy}	transverse shear stress (Pa)
ρ	mud density (kg/m^3)
λ	structure parameter (-)

ISSN 0867-7964 ISBN 978-83-7717-323-7 DOI 10.30825/4.12-28.2019

1. INTRODUCTION

Mine tailings are thickened to increase strength, save water and to accelerate consolidation to facilitate reclamation. Polymer addition emphasizes and accelerates these features, whilst ensuing pumpability. But what happens after exiting the pipe, before the material comes to rest? Where does the material go, what is the influence of changing material properties and how can the available storage space effectively be used? Doesn't flocculation compromise the formation of deposits through increased mud slopes? These are important questions that can be addressed by deposition modelling.

Where channel and lobe formation is a common feature in the deposition of thickened tailings, Charlebois (2012), Pirouz et al. (2015), the mechanisms behind their generation are little understood. In the laminar flow of thickened tailings, deposition occurs by two mechanisms: shear settling of sand (Talmon et al. 2014) and bed formation and stoppages of flow. Time-dependent rheological properties (such as thixotropy) are important to channel formation: likely leading to early stoppage of slow flows and channeling sheared-down material in faster streams. Our research question is therefore: can we quantify initial pattern formation in laminar deposition flow of tailings, muds and muddy debris flows? We only consider homogenous fluids (no shear settling of coarse) and do not consider routing by uneven terrain.

Our approach consists of an evaluation of the stability of the hydrodynamics by means of a linear stability analysis, followed by a back-analysis of governing physical processes from observations on channel formation in an existing flume test.

2. THEORY

A normal mode analysis is applied. It consists of a linearisation of the 2D gradual flow equations, and a subsequent substitution of harmonic perturbations for variations. The variations are quantified by sinusoidal and exponential functions.

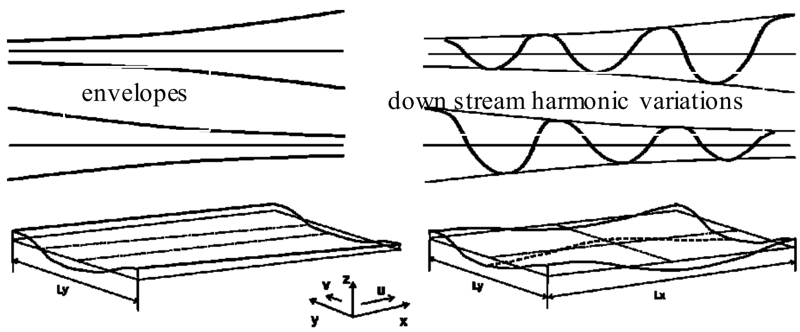

Figure 1. Definition sketches of harmonic perturbations of the mud level, highly exaggerated (equally applicable to spatial variation of horizontal flow velocities).

The base configuration is a uniform flow down an incline. The course of coupled infinitesimal variations of mud depth, longitudinal and transverse flow velocity is mathematically analysed: a normal mode analysis, like Struiksma et al. (1985). A definition sketch is given in Figure 1.

2.1 MATHEMATICAL DESCRIPTION

The equations for continuity, transverse flow (in concert with local mud slope) and longitudinal momentum are:

$$\frac{\partial h}{\partial t} + \frac{\partial uh}{\partial x} + \frac{\partial vh}{\partial y} = 0 \quad , \quad \frac{v}{u} = -\frac{\partial h}{\partial y}\Big/ i \quad , \quad -\rho g h (i - \frac{\partial h}{\partial x}) + \tau - \frac{\partial h \tau_{xy}}{\partial y} = 0$$

Closure relations for frictional processes are:

Bottom shear stress (already linearised): $\tau = \tau_0 \left(1 + n\frac{u'}{u_0} - n\frac{h'}{h_0} \right)$

Transverse shear stress: $\tau_{xy} = S \frac{\tau_0}{u_0 / h_0} \frac{\partial u}{\partial y}$

Decomposition of variables in a uniform ($_0$) , and a variable component (‘):

$$h = h_0 + h' \qquad u = u_0 + u' \qquad v = v'$$

The variable components are modelled by harmonic perturbations:

$$\left[\frac{u'}{u_0}, \frac{v'}{u_0}, \frac{h'}{h_0} \right] = \left[u, \tilde{\ }, .. \right] \; {}^{+bt} \left(\cos(my) + \mathrm{i}\sin(my) \right) + c.c.$$

with: $a = a_r + \mathrm{i}a_i$, $b = b_r + \mathrm{i}b_i$, consisting of real ($_r$) and imaginary ($_i$) contributions. Note:

$$e^{ax+bt} = e^{a_r x + b_r t} \left(\cos(a_i x + b_i t) + \mathrm{i}\sin(a_i x + b_i t) \right) + c.c.$$

Positive a_r represent perturbation profiles (or envelopes) which increase with distance, and positive b_r represent amplification in time. The imaginary part quantifies harmonic character: its relation to wave length of longitudinal harmonic perturbations is: $a_i = 2\pi/L_x$. Phase differences between variables are accounted for in the $u, \tilde{\ }, ..$ complex amplitudes of perturbations.

The resulting wave dispersion equation, which relates wave parameters a, b and m with physical parameters, is obtained by substitutions and rearrangement:

$$-(\frac{h_0 a}{i})^2 + \left(1 + 2n + S h_0^2 m^2\right)\frac{h_0 a}{i} + \left(\frac{b h_0}{u_0 i} + \frac{{h_0}^2 m^2}{i^2} \right)\left(n + S h_0^2 m^2\right) = 0$$

This equation will be applied to create a regime map for pattern formation, and to analyse pattern formation conditions.

2.2 SHEAR STRESSES AND RHEOLOGY

Bed shear stress: The bottom shear stress is linearised according to the Oswald-Dewaele power-law model, but the value of n may represent a linear approximation of any rheological model. Coussot et al. (1993) classified different types of rheological behaviour. The flow curve of a regular shear thinning fluid (type I), described for instance by the power-law model, is shown in Figure 2. In case of strong thixotropy, the flow curve is not monotone rising anymore: at low shear rates the local slope of the equilibrium flow curve (EFC) is negative, see Figure 2. This type (IV) of behaviour has been measured for flocculated tailings, Mizani et al. (2017). Such behaviour is captured by a negative value of n in our analysis. Associated transient adaptation of the colloid structure, Moore (1959), is not included in our analysis.

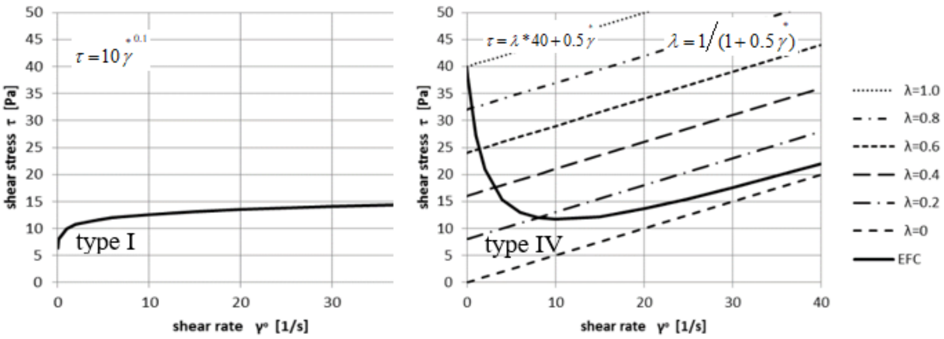

Figure 2. Examples of flow curves (EFC) for perturbation analysis: with and without thixotropy.

Transverse shear stress: The transverse shear stresses are modelled via a dimensionless horizontal viscosity S. Quantification comes with uncertainty and ideally it should reflect local rheology determined by the main flow. For reference, for laminar flow of constant viscosity fluids its value is S=1/3 as per definition of the bulk shear rate in open channels. With shear thinning fluids its value is expected to be higher, governed by conditions higher in the mud column. Its maximum value is determined by the necessity that side wall shear stresses do not exceed the bottom shear stress in the asymptotic case of fully developed channel flow (at max, considering the stagnant parts and the symmetry of perturbations, the perturbation velocity u' equals base velocity u_0): $S = (1+n)/(h_0 m)$.

3. ANALYSIS OF FLUME TEST

Our approach is to back-calculate the frictional/rheological parameters from observed wave pattern in order to understand the conditions for pattern formation when hydrodynamic processes are dominant.

3.1 FLUME TEST

Sisson et al. (2012) reported on a 3 h duration flume test (length 25 m, width 1 m) with laminar flow of slowly segregating prototype tailings at a mine site in Frt McKay, in Canada. The tailings are discharged (4.5 l/s) from an open-end pipe situated 1 m above the floor of the flume. An inclined wooden ground slope was installed in the flume, slope i=0.007. In the upstream 1 m there is a depression to accommodate the formation of a plunge pool. The test is started with an empty and clean flume configuration. After about 10 minutes of initial full width channel flow, one single channel formed in the middle of the flume, not exactly straight. After another 10 minutes, at a mud depth of about 0.1 m, a strongly asymmetric flow pattern developed, which consisted of temporally stagnant parts occupying half of the flume width. After some time the channel and stagnant parts could swap their position to the other side wall, by remobilisation of the stagnant part (cycle ~ 5 minutes). This observation is basically a slowly traveling 2D wave pattern (wavelength ~ 15 m). The question is, can we capture this with our non-segregating flow theory? Observed flow pattern are shown in Figure 3. Tailings density ~1700 kg/m^3, Oswald-DeWaele power-law approximation of the tailings's flow curve: n=0.1 (measured without sand, but this is not expected to influence n much).

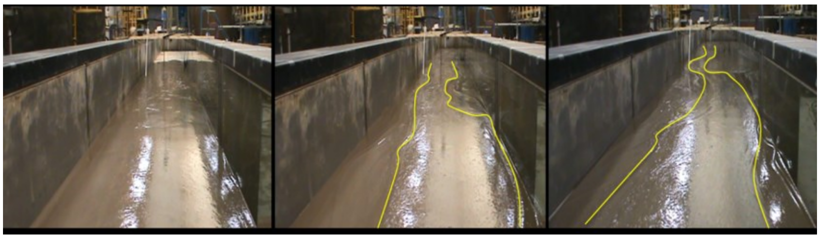

Figure 3. Laboratory flume trial of oil sands non-segregating tailings (NST) deposition. From left to right: full-width flow; formation of a single channel; meandering of the channel with lateral bars shifting downstream.

With respect to the wave dispersion equation, the dimensionless parameters of the observed wave pattern are:

- Normalised dimensionless celerity: $b_i h_0/u_0/i$ = - 0.05/0.007 = -7.
- Normalised dimensionless downstream wave length: $h_0 a_i/i$ = 0.04/0.007 = 5.7.
- Normalised dimensionless transverse wave length: $h_0 m/i$ = 0.1*π/0.007 = 45.

This corresponds to the broadest harmonic variation that can be accommodated between the flume's side walls.

3.2 REGIME MAP

A regime map is created on basis of the wave dispersion equation, for $h_0 m/i$=45, see Figure 4. Inspection of the dispersion equation reveals that the observed dimensionless celerity is negligible compared to transverse wave term, which allows a steady state approach. Lines (a_i) representing constant wave length and lines (a_r) representing constant adaptation length are plotted. Short longitudinal waves are not described by the theory because the transverse momentum balance has been simplified and acceleration/deceleration effects are not considered. Therefore $|h_0 a_i/i|$>10 conditions are not applicable to the analysis of this particular flume test.

The thick down-diagonal describes conditions where the influence of velocity variations on hydrodynamic friction is zero: $n+S(h_0 m)^2=0$. At and above this down-diagonal line straight channels are found (limited length). On the down-diagonal the two solutions are: $h_0 a_r$/i=1+n which describes a gently increase of perturbations with distance and a_r=0; an infinitely long straight channel. Below this down-diagonal there is no net restoring force for velocity variations in the momentum equation.

Below the down-diagonal line harmonic waves are predicted. In both area lines of constant downstream amplification rate are plotted. Above the down-diagonal these run parallel with this diagonal and can have a positive or negative value. Values vary progressive with distance to the down-diagonal. The longer channels are therefore found at or very close to the down-diagonal. The lines change their orientation below the down-diagonal and amplification factors do not vary as progressive as above the diagonal.

Harmonic waves are only found below the diagonal, associated lines of constant wave length are orientated parallel to this diagonal. The conditions of the flume test are therefore expected to be situated below the down-diagonal. Note that for positive n (no thixotropy) no harmonic waves are expected.

The adaptation length in the flume test cannot be quantified from the visual observations, a decent estimate is a range of: $-0.4 < h_0a_r/i < 0.4$ (the associated adaptation length of ~ 35 m is of the order of the flume length). With a reference value of S=1/3, the horizontal coordinate of the flume test in the regime plot is: $S(h_0m)^2$ =0.03. Its maximum value is a factor 10 higher. So the hydrodynamic conditions are at the left hand side of the regime map. Given the measured wave length, the associated value of n in the test is expected in the range $-0.3<n<-0.04$: which effectively represents thixotropic behaviour.

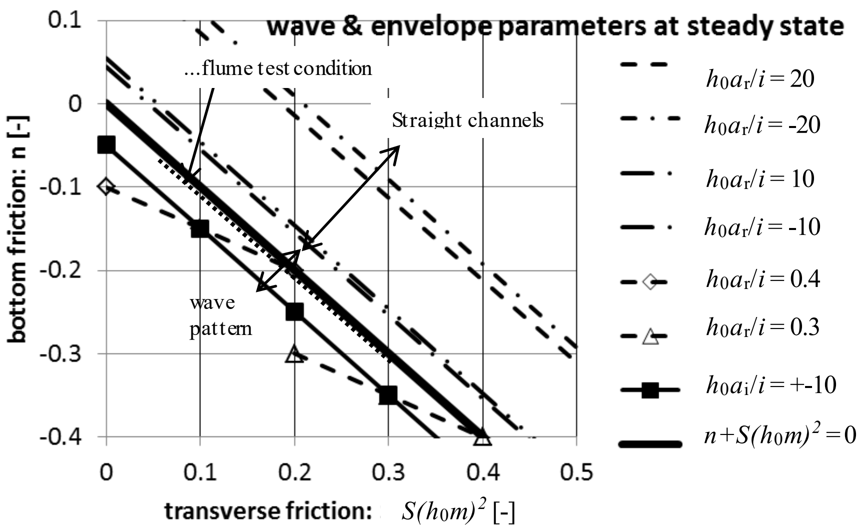

Figure 4. Regime map for Frt Mckay flume test (created for h0m/i=45).

3.3 FLUME SIDE WALLS

Wall friction with glass side wall panels is though not taken into account in the mathematical model, which is aimed at unrestricted conditions. But looking at the regime map, the influence of side walls can be understood: the low velocity parts, stuck to the walls, are subject to higher friction forces, so macroscopically there is an adverse relation between flow velocity and friction force, analogue to thixotropy, see Figure 5. We schematically can add the side wall friction (of the order of the yield stress), to the bottom friction of the low velocity part. With an already low positive n, as measured in the viscometry, the bottom shear stress in the high velocity stream will, in the analytical model, be smaller than the bed shear stress of the low velocity region in this truncated concept. In our model concept this boils down to thixotropy (= negative n).

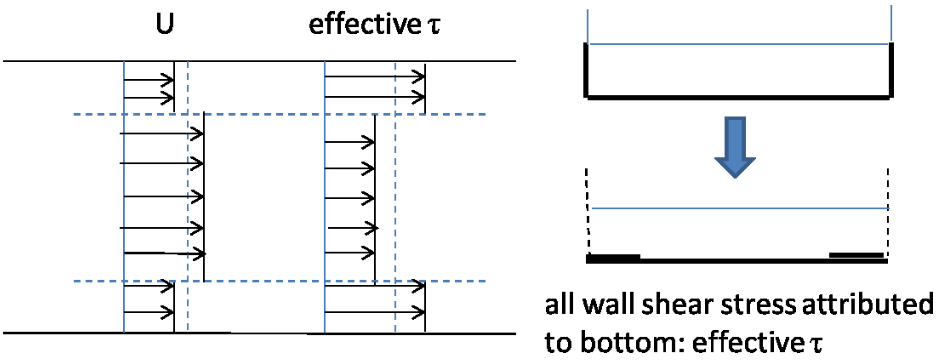

Figure 5. Analogy of influences of side wall shear stresses and thixotropy (adverse relation between variation of flow velocity and variation of bed shear stress)

4. RESEARCH NEEDS ANALYTICAL PATTERN MODELLING

As already mentioned, the regime map contains an area with harmonic waves. It is the expectation that transient adaptation of colloid structure and rheology, Moore (1959), will lead to a modification of the size and location of this harmonic wave area (positive n should in that case be applied, since type IV behaviour is then described by a combined variation of the structure parameter λ and variation of shear rate).

The flume test displayed morphodynamic behaviour, which is revealed by the slow rise of mud level and dynamic variation of remobilisation. Sand deposition is expected to enhance the time-dependency of meandering: strongest depositions occur within the channel. The channel clogs steadily and the pattern will shift its position. The linearised hydrodynamics need to be coupled with linearised gelled bed formation theory to see if/how this produces harmonic 2D patterns and channels.

5. CONCLUSIONS

A basis is laid for the analysis of pattern/channel formation in free surface flow of shear thinning fluids. Decisive to pattern formation are the friction parameters n and S. In hydrodynamic context, meandering/braiding only occurs when velocity variations are not opposed by net frictional damping. Straight channel formation occurs when velocity variations are marginally opposed by net frictional resistance. In both cases the material is to behave thixotropic. Stronger thixotropy can lead to meandering/braiding. Such channels and patterns are expected to have limited length. Side-walls presence in flume testing may lead to pattern formation, comparable to thixotropy influences. The approach needs to be extended with transient adaptation of colloid structure to better capture thixotropy. The flume test displayed morphodynamic behaviour, which is revealed by the slow rise of mud level and dynamic variation of remobilisation. Therefore a similar analysis has to be conducted which includes consequences of (gelled) bed formation by settling sand.

ACKNOWLEDGEMENTS

The author would like to thank IOSI and COSIA of Canada for supporting development of deposition modelling. Thanks to Dick Mastbergen for post-processing video material.

REFERENCES

1. Charlebois, L.E., 2012, On the flow and beaching behaviour of sub-aerially deposited, polymer-flocculated oil sands tailings: a conceptual and energy-based model, MASc-thesis, The University of British Columbia.
2. Coussot, P., Leonov, A.I., Piau, J.M., 1993, Rheology of concentrated dispersed systems in a low molecular weight matrix, Journal of Non-Newtonian Fluid Mechanics, 46, 179-211.
3. Mizani, S., Simms, P,. Wilson, W., 2017, Rheology for deposition control of polymer-amended oil sands tailings, Rheol Acta, DOI 10.1007/s00397-017-1015.
4. Moore, F., 1959, The rheology of ceramic slips and bodies, Transactions British Ceramic Society, 58, 470-494.
5. Pirouz, B., Javadi, S., Williams, P., Pavissich, C., Caro, G., 2015, Chuquicamata Full-Scale Field Deposition Trial, Paste 2015, Cairns.
6. Sisson, R., Lacoste-Bouchet, P., Vera, M., Costello, M., Hedblom, E., Sheets, B., Nesler, D., Solseng, P., Fandrey, A., Van Kesteren, W.G.M., Talmon, A.M., Sittoni, L., 2012, An analytical model for tailings deposition developed from pilot-scale testing, 3rd International Oil Sands Tailings Conference, Edmonton, Alberta, Canada, December 2-5, 2012, 53-63.
7. Struiksma, N., Olesen, K.W., Flokstra C., de Vriend, H.J., 1985, Bed deformation in alluvial channel bends, J. Hyd. Res., 23(1), 57-79.
8. Talmon A.M., van Kesteren, W.G.M., Sittoni, L., Hedblom, E., 2014, Shear cell tests for quantification of tailings segregation, Canadian J. Chemical Engineering, 92, 362-373.